AAPS PharmSciTech, Vol. 11, No. 1, March 2010 (© 2010)
DOI: 10.1208/s12249-010-9390-3

Research Article

Insulin-Loaded Nanoparticles Based on *N*-Trimethyl Chitosan: *In Vitro* (Caco-2 Model) and *Ex Vivo* (Excised Rat Jejunum, Duodenum, and Ileum) Evaluation of Penetration Enhancement Properties

Giuseppina Sandri,[1] Maria Cristina Bonferoni,[1] Silvia Rossi,[1] Franca Ferrari,[1] Cinzia Boselli,[2] and Carla Caramella[1,3]

Received 28 September 2009; accepted 1 February 2010; published online 16 March 2010

Abstract. The aim of this paper was to evaluate the penetration enhancement properties of nanoparticles (NP) based on *N*-trimethyl chitosan (TMC 35% quaternization degree) loaded with insulin. The permeation performances of TMC NP were compared with those of chitosan (CS) NP and also with TMC and CS solutions. To estimate the mechanism of penetration enhancement, two different approaches have been taken into account: an *in vitro* study (Caco-2 cells) and an *ex vivo* study (excised rat duodenum, jejunum, and ileum). Insulin-loaded CS and TMC NP had dimensions of about 250 nm and had high yield and high encapsulation efficiency. The *in vitro* study evidenced that TMC and CS were able to enhance insulin permeation to the same extent. Penetration enhancement properties of TMC NP seem to be prevalently related to endocytosis while the widening of tight junctions appeared more important as mechanism in the case of CS NP. The *ex vivo* study put in evidence the role of mucus layer and of its microclimate pH. In duodenum (pH 5–5.5), CS and TMC solutions were more effective than NP while TMC NP were more efficient towards jejunum tissue (pH 6–6.5) for their high mucoadhesive potential. Confocal laser scanning microscopy study supported the hypothesis that penetration enhancement due to TMC NP was mainly due to internalization/endocytosis into duodenum and jejunum epithelial cells. The good penetration enhancement properties (permeation and penetration/internalization) make TMC NP suitable carriers for oral administration of insulin.

KEY WORDS: absorption properties; caco-2 model; *ex vivo* rat intestine model; insulin; internalization/uptake; trimethyl chitosan nanoparticles.

INTRODUCTION

The research in biotechnology and biochemistry has led to the discovery of peptides and proteins characterized by strong biological activity. However, the administration of therapeutically active peptides/proteins has been almost exclusively limited to the parenteral route, and the administration via oral route still represents one of the greatest challenges in the pharmaceutical/technological field. The successful delivery via oral route is impaired by the permeation/absorption difficulties due to the high molecular weight and the hydrophilicity of the peptidic molecules and their extensive enzymatic degradation due to proteases before reaching the site of absorption (1). The intestinal epithelium regulates the passage of natural compounds and acts as a barrier for paracellular passive transport of large hydrophilic molecules. This absorption barrier is composed of a single layer of columnar epithelial cells joined at the apical surface by a tight junctional complex. The junctional complex forms a continuous seal, which segregates the apical from the basolateral compartment and conveys size and charge selectivity due to the presence of negative charge in its structure (2). However, oral route is considered to be the most suitable and convenient one for chronic therapies such as those with employing insulin in the case of diabetes (1).

Nanoparticulate carriers represent a very promising drug delivery platform to deliver peptidic drugs via oral route because they are stable in physiological fluids and are able to protect the drug from adverse conditions of the gastrointestinal tract and to control drug release (3). The success of this approach relies on a number of interesting properties, namely, mucoadhesion properties conceivably related to the combination of the particle size and the particle superficial charge (4), a high capacity to associate and release therapeutic macromolecules in the bioactive form, as well as the ability to enhance the transport of bioactive compounds across well-organized epithelial barriers, such as the intestinal one. Mucoadhesive properties play an important role in oral drug delivery systems by prolonging the residence time of drug carriers and also

[1] Department of Pharmaceutical Chemistry, School of Pharmacy, University of Pavia, viale Taramelli 12, 27100, Pavia, Italy.
[2] Department of Applied and Experimental Pharmacology, University of Pavia, viale Taramelli 14, 27100, Pavia, Italy.
[3] To whom correspondence should be addressed. (e-mail: carla.caramella@unipv.it)

increasing the intimacy of contact between drug and mucus membrane at the absorption sites, therefore enhancing the permeability and reducing the degradation of drugs (5). There is a strong belief that nanoparticles (NP) of appropriate size can pass intact the mucosal membranes and deliver the loaded drug into the systemic circulation (2). Several proof-of-concept studies have consistently demonstrated the efficacy of mucoadhesive nanoparticles in various animal models (6).

Chitosan (CS) is a polycationic linear polysaccharide (1-4)-linked 2-amino-2-deoxy-D-glucose and residual 2-acetamido-2-deoxy-D-glucose. CS is known to be biodegraded by several enzymes. Among them are chitinases, which are secreted by intestinal microorganisms, and lysozyme, which is highly concentrated in mucosal surfaces and by human chitotriosidase (6). CS is firmly established as a biocompatible nontoxic mucoadhesive polymer that exhibits the capacity to promote the absorption of poorly absorbed macromolecules across epithelial barriers by transient widening of cell tight junctions. CS has a pK_a of about 6.5, and it loses its charge and precipitates in neutral and basic environments as prevailing in the intestine. Studies have shown that only protonated soluble chitosan in its uncoiled configuration can trigger the opening of the tight junctions and facilitate the transport of hydrophilic compounds (2). Hence, CS can be used as an enhancer only in the proximal part of the intestine where the pH is close to its pK_a value. Subsequently, quaternized derivatives of chitosan, synthesized by introducing various alkyl groups to the NH_2 groups of the chitosan molecule structure, were extensively studied. These derivatives are drastically more soluble in neutral and alkaline environments of the intestine and hence are more efficient than chitosan for drug delivery and absorption across the intestinal epithelium of the jejunum and ileum (7,8). The permeation-enhancing properties of these chitosan derivatives have been attributed to their ionic interactions with the tight junctions and cellular membrane components to increase the paracellular permeation of hydrophilic compounds (8). The chitosan derivatives in nanoparticle form have less positive surface charge because part of the basic groups is involved in the cross-linking reaction with tripolyphosphate (TPP). Their interactions with tight junction are therefore limited, and hence the drug transport across the monolayer more likely occurs through the transcellular pathway rather than by tight junction opening (2).

Recently, nanoparticles based on *N*-trimethyl chitosan chloride (TMC) were proved to interact with intestinal tissue (rat jejunum) and with Caco-2 cell monolayers (9). In particular, the increase in quaternization degree of trimethyl chitosan favored the mucoadhesion. In addition, the TMC nanosystems were able to improve the permeability of fluorescein isothiocyanate (FITC)-labeled dextran (FD4; MW 4,400 Da) and the nanosystems based on TMC fully quaternized demonstrated to be entrapped into rat intestinal tissue and into Caco-2 cell monolayers (2).

TMC nanosystems with 35% quaternization degree combined good penetration enhancement properties and mucoadhesion: even if the mucoadhesive properties slowed down the absorption of nanoparticles through the mucus layer into the cell, the increase of the contact with the intestinal epithelium offered more possibilities for nanoparticle internalization (2).

Given these premises, the aim of this paper was to evaluate the penetration enhancement properties of nanoparticles based on TMC (35% quaternization degree; TMC NP) loaded with insulin. The permeation performance of TMC NP was compared with that of CS NP and also with TMC and CS solutions. To estimate the mechanism of penetration enhancement, two different approaches have been taken into account: an *in vitro* model (Caco-2 cells) and an *ex vivo* methodology (excised rat duodenum, jejunum, and ileum). Moreover, NP internalization/uptake into excised rat jejunum, duodenum, and ileum was evaluated by means of confocal laser scanning microscopy (CLSM).

MATERIALS AND METHODS

Materials

TMC, having quaternization degree of 35%, was obtained from a 90% deacetylated chitosan (MW 580 kDa) from shrimp (CS; Chito-clear FG90, Primex, Siglufjordur, Iceland), using procedures described in the literature (10), and was previously characterized by Di Colo *et al.* (11). Pentasodium tripolyphosphate (TPP; Sigma, Milan, Italy) was used as TMC and CS cross-linking agent.

Fluorescein isothiocyanate insulin (fluorescent-labeled; FL-INS; Sigma, Milan, Italy) was used.

All the reagents were of analytical grade (Sigma-Aldrich, Milan, Italy).

Methods

Polymer Solution Preparation

TMC and CS were hydrated in HCl 0.01 N under stirring at room temperature. Each polymer solution (ps) had 1.67 mg/ml polymer concentration and 155.6 μg/ml insulin concentration.

Nanoparticle Preparation

CS and TMC NP were prepared according to the mild operation procedure developed by Calvo *et al.* (12) based on ionotropic gelation of TMC and CS (polycations) with TPP polyanion as previously assessed (9). The ionotropic gelation takes place when the positively charged amino groups of TMC and CS interact with the negatively charged TPP. TMC or CS was dissolved at 2.5 mg/ml in distilled water by means of gentle stirring, while TPP was dissolved at 2.5 mg/ml in distilled water.

FL-INS was solubilized in HCl 0.01 N at 1-mg/ml concentration. TPP was solubilized in water at 2.5-mg/ml concentration.

Seven hundred microliters of insulin solution was added to 3 ml of each polymer solution under stirring; subsequently, TPP solution was added to obtain a final volume of 4.5-ml nanoparticle suspensions. Nanoparticle suspensions were maintained under stirring at room temperature for 30 min to stabilize the systems.

The nanoparticulate systems were characterized by the following compositions: insulin 155.56 μg/ml; TMC and CS 1.67 mg/ml; TPP 0.42 mg/ml for TMC system and 0.28 mg/ml for CS system. FL-INS concentrations were the same for all nanoparticles, polymer solutions, and reference FL-INS solution.

Nanoparticle Characterization

Particle size was measured at 25°C by Photon Correlation Spectroscopy (Beckman Coulter N5; Instrumentation

Laboratory, Milan, Italy) at an angle of 90° after dilution of formulations with bidistilled and filtered (0.45 μm, Millipore, Vimodrone, Italy) water. Each sample was measured in triplicate.

The manufacturing yield of each nanoparticulate system was calculated following the procedure described below. Each nanoparticle suspension was centrifuged at 10,000×*g* for 30 min; the supernatant was removed. The precipitated nanoparticles were then rinsed twice with distilled water and freeze-dried (Powerdry LL 1500-55, Heto, Analitica De Mori, Milan, Italy). The yield% was calculated as the ratio between the freeze-dried sample weight and the theoretic weight.

The encapsulation efficiency (EE%) of FL-INS was calculated as follows: first, the amount of drug associated with nanoparticles was calculated as the difference between the total amount of FL-INS added to the system called FL-INS_t (theoretic) and FL-INS recovered in the supernatant assuming that the FL-INS not recovered in the supernatant was encapsulated in the nanoparticles. Subsequently, the ratio between FL-INS encapsulated in nanoparticles and the nanoparticle amount (yield) was calculated and expressed as percentage, according to the following equation:

$$EE\% = (\text{FL-INS}_t - \text{FL-INS}_s)/NP \times 100$$

Where

FL-INS_t = FL-INS theoretic amount employed for nanoparticle preparation
FL-INS_s = FL-INS free amount recovered in the supernatant
NP = amount of nanoparticles derived using manufacturing yield

FL-INS remaining in the supernatant or loaded into the nanosystems was assayed by means of high-performance liquid chromatography (HPLC) method adapted from (13) as here described at the following conditions. A C_8 column (Zorbax-R_X-C8 (2 μm 150×4.6 mm), Agilent, Bischoff, D) was used as stationary phase; the mobile phase consisted of 2.5 mM KH_2PO_4 pH 3 (60%) and acetonitrile (40%) at 1 ml/min; the injection volume was 10 μl, and the fluorimetric detection was at the following wavelength: λ_{ex}=490 nm and λ_{em}=515 nm.

The method was validated according to ICH guideline entitled "Validation of analytical procedures: text and methodology" Q2(R1), version 4. The method was demonstrated to be linear (R^2>0.999), accurate (recovery%±2%), and precise (intraday and interday precision calculated as relative standard deviation < ± 2%).

The EE% of FL-INS was calculated as the ratio between FL-INS loaded into the nanoparticulate systems with respect to the total amount of FL-INS employed for nanoparticle preparation as follows (9):

$$EE\% = (\text{FL-INS}_t - \text{FL-INS}_s)/\text{FL-INS}_t \times 100$$

Where

FL-INS_t = FL-INS theoretic amount employed for nanoparticle preparation
FL-INS_s = FL-INS free amount recovered in the supernatant.

Nanoparticle Stability and Stabilization

CS and TMC nanosystems were subjected to evaluation of particle size by means of photon correlation spectroscopy (PCS) immediately after the preparation, after storage for 1 week at 2–8°C and after freeze-drying and resuspension in distilled water at the starting concentration.

Cytotoxicity

Caco-2 cells were seeded in 96-well plates with area of 0.34 cm^2 at density of 10^5 cells per square centimeter. After 7 days, the growing cells attached to the well bottom composed of a monolayer, and at the eighth day the experiments were performed. The toxicity study was performed using the neutral red (NR) assay (Tox Kit 4, Sigma-Aldrich, Milan, Italy) that determines the accumulation of the neutral red supravital dye in the lysosomes of viable, uninjured cells. Cell membrane or lysosome damages cause a poor capability or no capability to pick up NR.

Each well was washed with saline phosphate buffer (PBS) and 500 μl of each sample (diluted 1:1 with Hank's Balanced Salt Solution (HBSS; $CaCl_2$ anhydrous 140 mg/l, $MgCl_2$ $6H_2O$ 100 mg/l, $MgSO_4$ $7H_2O$ 100 mg/l, KCl 400 mg/l, KH_2PO_4 60 mg/l, $NaHCO_3$ 350 mg/l, NaCl 8,000 mg/l, Na_2HPO_4 48 mg/l, D-glucose 1,000 mg/l, Phenol Red 10 mg/l; Sigma, Milan, Italy)) at pH 5.5 was put in contact with the cells (the same sample concentration and the same sample amount/area ratio were maintained as used in permeation experiment across Caco-2 cells). After 2 h, the samples were removed and the cell substrates washed with PBS. Two hundred microliters of NR solution (0.33 mg/ml in Dulbecco's modified Eagle's medium (DMEM)) was put in each well for either 1 or 2 h of contact time. Cell substrates were then washed with PBS to remove NR not entrapped in the cells, and the fixing medium (1% $CaCl_2$ and 0.5% formaldehyde aqueous solution) was added to fix the substrate. After removal of the fixing solution, a solubilizing solution (1% of acetic acid in ethanol) was added to the cell substrates to cause cell disruption and to release NR captured by viable cells. The NR solution absorbance was determined by means of a plate reader (Perkin Elmer, Milan, Italy) at wavelength of 490 nm. The absorbance read for each sample was compared with that of HBSS, negative control, that is not toxic and that was assumed to allow maximum cell viability (100%).

Permeability Studies Performed by Means of Caco-2 Cells

The nanoparticle suspensions were diluted 1:1 using pH 5.5 HBSS and were subjected to permeability tests across Caco-2 cell monolayers.

Caco-2 cells (TC7; passage 37) were seeded on tissue-culture-treated polycarbonate filters (area 113.1 mm^2; inner diameter 13.85 mm, pore size 0.4 μm) in 12-well plates (Greiner Bio-one, PBIinternational, Milan, Italy) at seeding density of $2.5.10^5$ cells per square centimeter. DMEM (pH 7.40; Bioindustries, PBIinternational, Milan, Italy) supplemented with 10% fetal bovine serum, benzylpenicillin G (160 U/ml), and streptomycin sulfate (100 μg/ml; Bioindustries, PBIinternational, Milan, Italy) and also with

1% nonessential amino acids (Sigma, Milan, Italy) was used as culture medium. Cell cultures were kept at 37°C in an atmosphere of 95% air and 5% CO_2 and 95% of relative humidity. Filters were used for transepithelial electrical resistance (TEER) measurements and transport experiments 21–23 days after seeding.

Five hundred microliters of the nanoparticle suspensions was diluted 1:1 in HBSS at pH 5.5 and were used as the apical (donor) phase of the monolayers. HBSS at pH 7.4 (2 ml) was used as the basolateral (receptor) phase and added to the basolateral side of the monolayers. At 0.5, 1, and 2 h, each filter and its mounting donor chamber filled with the apical phase were moved into a fresh basolateral (receptor) phase. All the receptor phases were collected, and FL-INS permeated was assayed by means of HPLC method previously described. After 2 h, the apical and the basolateral phases were withdrawn, and each Caco-2 monolayer was rinsed and put in contact with a Lucifer Yellow (LY, Sigma-Aldrich, Milan, Italy) solution at 25 μg/ml in HBSS and fresh HBSS as basolateral phase. After 1-h contact time, the permeated LY was assayed by means of a spectrofluorometric method (λ_{ex}=428 nm; λ_{em}=521 nm). The apparent permeability coefficient (P_{app}) was calculated using the following equation (8):

$$P_{app} = dQ/dt/(A \cdot 60 \cdot C_0)$$

where

dQ/dt = permeability rate (drug amount permeated per minute)
A = diffusion area of the monolayer
C_0 = initial FL-INS or LY concentration

The FL-INS recovery was subsequently calculated according to the following equation:

$$\%\text{FL-INS recovery} = \left(\text{FL-INS}^{t3}_{apical} + \text{FL-INS}^{t3}_{basolateral}\right)/\text{FL-INS}^{t0}_{apical} \times 100$$

where

$\text{FL-INS}_{apical}^{t3}$ = amount of FL-INS remained in the apical phase at the end of the permeation experiment (2 h)
$\text{FL-INS}_{basolateral}^{t3}$ = amount of FL-INS recovered in the basolateral phase at the end of the permeation experiment (2 h)
$\text{FL-INS}_{apical}^{t0}$ = amount of FL-INS present in the apical phase at the beginning of the permeation experiment (2 h)

During the experiments, the integrity of the monolayers was assessed by means of TEER measurements at fixed times using a Millicell ERS-meter (Millipore Corp., Bedford, MA, USA).

Permeation Measurements Across Excised Rat Duodenum, Jejunum, and Ileum Tissues

All animal experiments were conducted in full compliance with the standard international ethical guidelines (European Communities Council Directive 86/609/EEC) approved by the Italian Minister of Health (D.lgs.vo 116/92). The protocol of the study was approved by the Local Institutional Ethics Committee for the use of animals in research of the University of Pavia.

The nanoparticle suspensions and the polymer solutions were diluted 1:1 with HBSS buffered at pH 5.5. These samples were subjected to permeation measurement by means of Franz diffusion cells with a 20-mm orifice diameter (3.14-cm^2 diffusion area) and 15-ml volume (Permeagear, Hellertown, PA, USA) thermostated at 37°C. Fresh rat duodenum, jejunum, or ileum tissues excised by male Wistar-Harlan rats (body weight 250–350 g), laying on a filter paper, were placed between the donor and the acceptor chambers of the Franz diffusion cell. In the tissue preparation before the experiment, care was taken in order to preserve the mucus layer that covered the tissue, and moreover, the freshly excised duodenum and jejunum tissues were still secreting mucus during the experiment. Each sample was placed in the donor chamber on the luminal surface of rat intestinal tissues. pH 7.4 HBSS was used as acceptor phase (sink conditions in the acceptor phase were maintained during the test).

The permeation test was also performed by using FL-INS solution in HBSS pH 5.5, having the same concentration of the polymer samples as reference.

At fixed time intervals, 500-μl samples of the acceptor phase were withdrawn and replaced with fresh buffer. FL-INS was assayed by means of HPLC method as previously described.

The P_{app} was calculated using the equation previously reported (11).

The enhancement ratio (ER) was calculated for each sample as the ratio between the P_{app} obtained in the presence of CS or TMC as solutions or as nanoparticulate systems with respect to P_{app} obtained for insulin solution without penetration enhancer.

Evaluation of Nanoparticle Penetration into Excised Rat Duodenum, Jejunum, and Ileum Tissues with CLSM

At the end of each permeation experiments (2 h), each tissue was rinsed twice with pH 7.4 HBSS, included in the OTC compound (Leika Microsystem, Mannheim, Germany), frozen in liquid nitrogen, and stored at −80°C.

Slices perpendicular to the intestinal surface, 10 μm in thickness, were cut from duodenum, jejunum, and ileum after the permeation experiment, included in the OTC Compound (Leica Microsystem srl, Milan, Italy), using a cryostat (Leica CM1510, Leica Microsystem srl, Milan, Italy) at −20°C. Each slice was placed on a microscope slide, dehydrated for 12 h, and subsequently fixed by dipping the microscope slides in acetone.

The nuclei of cell monolayers and of the tissue slice were stained by dipping the biological substrates into a solution (1:10,000) of propidium iodide (Sigma, Milan, Italy).

Each microscope slide was mounted using polyvinyl alcohol mounting medium with DABCO antifading ((mixture of tris(hydroxymethyl)aminomethane, tris/hydroxymethyl) aminomethane hydrochloride, polyvinyl alcohol 22,000 Da, glycerol anhydrous and 1,4-diazabicyclo[2.2.2]octane; Bio-Chemika, Fluka, Milan, Italy) and covered with cover glass.

The slides were observed using a confocal laser scanning microscope using λ_{ex}=485 nm and λ_{em}=515 nm for the visualization of FL-INS and λ_{ex}=530 nm and λ_{em}=625 nm for the visualization of propidium iodide. The acquired images were processed by means of a software (Leica Microsystem srl, Milan, Italy). Fluorescence intensities were set up to avoid saturation.

Statistical Evaluation

Statistical differences were determined using one-way ANOVA and post hoc Sheffe tests for multiple comparisons (Siphar, Creteil, France). Differences between groups were considered to be significant at $p<0.05$.

RESULTS AND DISCUSSION

Characterization of Nanoparticles

Figure 1 reports particle size of blank and insulin-loaded CS and TMC nanoparticles. CS NP had dimensions of about 220 nm that are not significantly influenced by drug loading. TMC NP dimensions were about 250 nm comparable to those of CS NP for the blank system; in this case, a significant reduction of dimensions was observed after drug loading ($p<0.01$).

Figure 2 reports yield and encapsulation efficiency percent values for CS and TMC nanoparticles loaded with insulin. Both nanoparticulate systems showed high yield and encapsulation efficiency values: for CS NP, the yield was about 75% with an EE of about 79% and for TMC NP the yield is about 56% with an EE of about 94%. HPLC assay did not evidence insulin degradation.

The high encapsulation efficiency should protect insulin from enzymatic degradation due to peptidases and pH variations of the gastrointestinal tract (5).

Nanoparticle Stability and Stabilization

After 1 day of storage, both for CS NP and TMC NP, dimensions increased up to diameters higher than 3,000 nm (the upper detection limit of PCS apparatus): this indicated an irreversible aggregation of nanoparticles during storage probably caused by formation of strong interparticle and intraparticle bonding.

After freeze-drying, CS NP could not be easily resuspended. Freeze-dried TMC NP after resuspension was characterized by dimensions (268 nm; SD±7) not significantly different with respect to the freshly prepared ones. This indicated that lyophilization could be a suitable procedure to stabilize TMC NP.

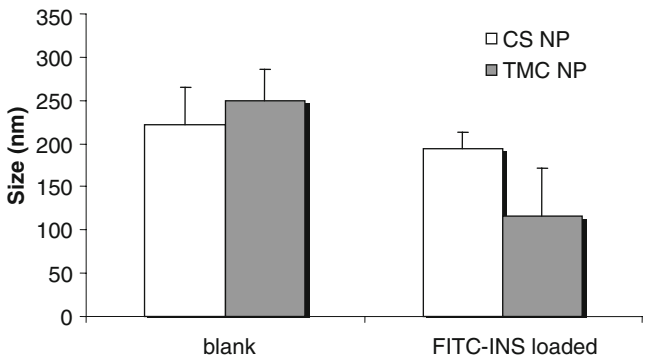

Fig. 1. Size (nm) of blank and FITC-INS-loaded nanoparticles based on CS and TMC (mean values ± SD; n=3)

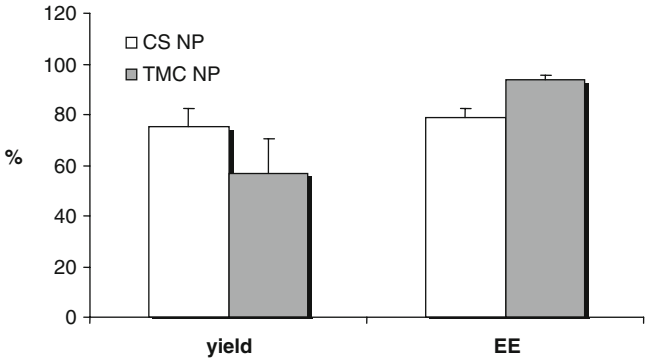

Fig. 2. Yield and encapsulation efficiency percent values for FITC-INS nanoparticles based on CS and TMC (mean values ± SD; n=3)

In Vitro Cytotoxicity and Permeability Study (Caco-2 Cells)

Figure 3 reports the results of cytotoxicity study as viability% evaluated for CS and TMC as polymeric solution (ps) and as NP.

For all the samples, biocompatibility was good (viability close to 100%) after both 1 and 2 h of contact time. This indicates that trimethylation (35%) did not change the biocompatibility of CS also in nanoparticulate form.

Figure 4 reports TEER% profiles as a function of time evaluated during permeability experiments for CS and TMC as ps and as nanoparticulate systems (NP) and for insulin solution (sol) as reference.

At the beginning of the permeation experiments, the mean TEER value was 550 Ωcm^2 (standard deviation ±25 Ω cm^2) to indicate the junctional integrity of Caco-2 cell monolayers. For insulin solution, TEER% profile remains almost close to 100% value during the experiment time to indicate that insulin as free molecule did not impair the permeability barrier of the Caco-2 monolayer *in vitro* and the paracellular pathway. All the polymeric samples caused a decrease of TEER profiles conceivably due to the capability of chitosan and its derivative to widen the paracellular route by interacting and interfering with junctional proteins of tight junctions (14,15). CS solution allowed a significant decrease of TEER value after a time as short as 30 min to indicate a ready action while TMC took longer time to induce the same effect. Not only polymer

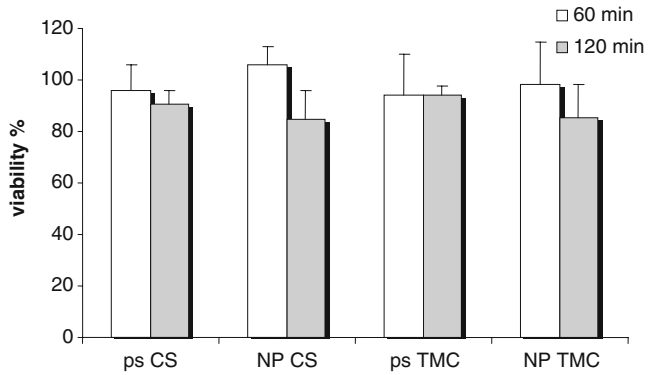

Fig. 3. Cytotoxicity values (viability%) evaluated for chitosan (*CS*) and trimethyl chitosan (*TMC*) as polymeric solution (*ps*) and as nanoparticulate systems (*NP*) (mean values ± SD; n=8)

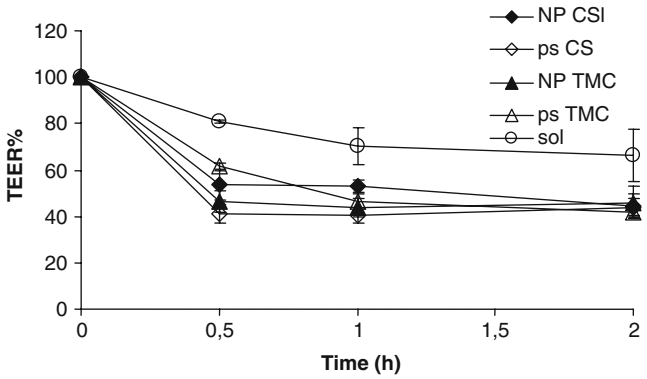

Fig. 4. TEER% profiles as a function of time evaluated during permeability experiments for chitosan (*CS*) and trimethyl chitosan (*TMC*) as polymeric solution (*ps*) and as nanoparticulate systems (*NP*) and for insulin solution (*sol*) as reference (mean values ± SD; $n=6$)

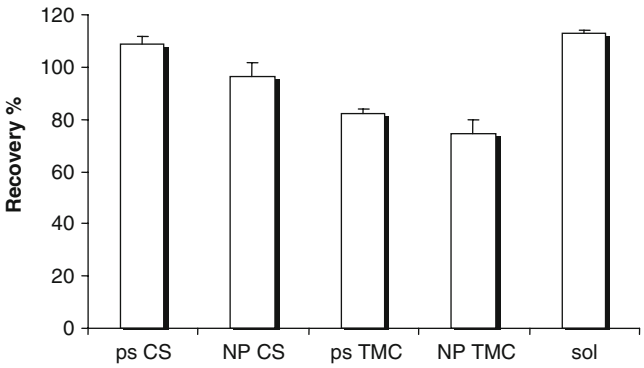

Fig. 6. Recovery% values of insulin in Caco-2 cell monolayers after the contact with chitosan (*CS*) and trimethyl chitosan (*TMC*) as polymeric solution (*ps*) and as nanoparticulate systems (*NP*) and insulin solution (*sol*) as reference (mean values ± SD; $n=6$)

solutions but also nanoparticulate systems were able to determine a decrease of TEER values suggesting a modulation of the cell junction integrity. This is in agreement with the results previously reported by Ma and Lim (16).

Figure 5 reports P_{app} values calculated for insulin (ins) and LY and enhancement ratio of insulin (ER) for CS and TMC as ps and as NP and insulin sol as reference.

CS and TMC as nanoparticles and as polymeric solutions determined P_{app} value higher than that of insulin solution ($p<0.05$) to indicate that all the polymeric samples enhanced insulin permeation. CS NP showed highest P_{app} value followed by TMC and CS as polymeric solutions and TMC NP, even if no significant differences could be evidenced between polymeric samples. The values of ER confirmed P_{app} trend and evidenced that the system based on CS as nanoparticles was able to increase insulin permeation up to twofold. TMC both as polymeric solution and nanoparticles allowed permeation of LY to the same extent as insulin solution, indicating that TMC did not influence the integrity of paracellular pathway in accordance with the slowest effect of TMC in opening the tight junctions. On the contrary, CS as solution and especially as NP caused P_{app} value for LY significantly greater than TMC samples ($p<0.05$), suggesting a quick widening of tight junctions.

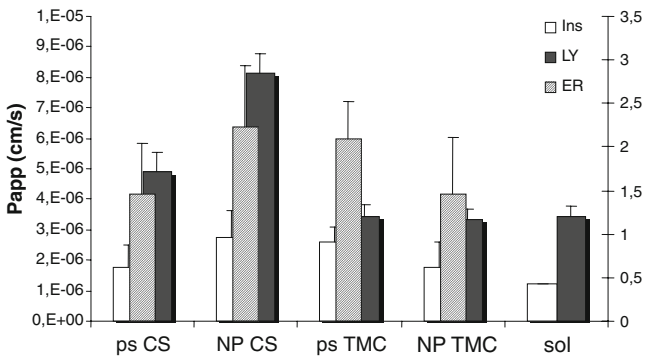

Fig. 5. P_{app} values calculated for insulin (*ins*) and Lucifer yellow (*LY*) and enhancement ratio of insulin (*ER*) for chitosan (*CS*) and trimethyl chitosan (*TMC*) as polymeric solution (*ps*) and as nanoparticulate systems (*NP*) and insulin solution (*sol*) as reference, obtained using Caco-2 cell substrate (mean values ± SD; $n=6$)

Figure 6 reports the recovery% values of insulin calculated after the contact with CS and TMC as ps and as NP. Insulin sol was given as reference. CS polymeric solution and NP determined insulin recovery% not significantly different and close to 100% to indicate that insulin permeated across cell substrate and was not taken up by the cells. On the contrary, TMC solution and NP determined insulin recovery significantly lower ($p<0.05$) than 100% and than those of CS samples to indicate that insulin was partially entrapped into cells. This suggests that TMC with 35% trimethylation should preferentially determine transcellular transport of insulin rather than paracellular one.

Permeation Measurements Across Excised Rat Duodenum, Jejunum, and Ileum Tissues

Figure 7 shows P_{app} (cm/s) values of FL-INS calculated from permeability experiments performed using excised rat duodenum, jejunum, and ileum with TMC NP and CS NP, with the corresponding polymer solutions and with FL-INS sol as reference.

All the polymeric samples, both as solution and as NP, were characterized by P_{app} values of FL-INS much higher than that of FL-INS sol towards rat duodenum and jejunum ($p<0.05$), allowing enhanced permeation of insulin across these intestine tracts.

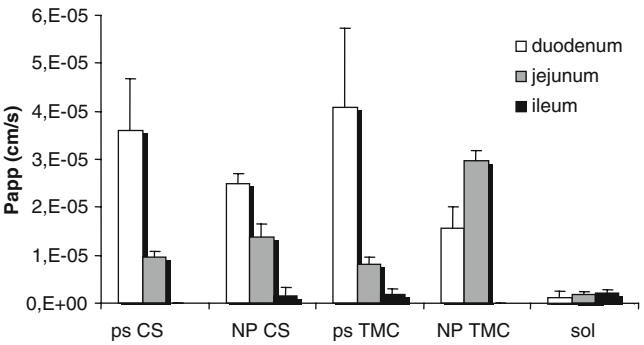

Fig. 7. P_{app} values (cm/s) of insulin calculated for TMC and CS nanoparticulate systems, TMC and CS polymer solutions, and insulin solution as reference obtained using excised duodenum, jejunum, and ileum (mean values ± ES; $n=6$)

In the duodenum, CS and TMC solutions were able to enhance the permeation of insulin to a greater extent with respect to the corresponding NP ($p<0.05$). No significant differences were evident between the performance of TMC and CS, indicating that the trimethylation of CS did not improve penetration enhancement properties. Such behavior was also previously described for some chitosan derivatives (TMC, dimethyl ethyl chitosan, diethyl methyl chitosan, and triethyl chitosan with degree of substitution of approximately 50±5%) by using an *in vitro* model, Caco-2 cell monolayer (2).

In the jejunum, TMC NP and CS NP showed higher penetration enhancement properties than those of the corresponding polymer solutions. Even if TMC and CS performances were comparable in the case of polymer solutions, TMC NP was more effective than CS NP in these conditions ($p<0.05$).

TMC NP did not suffer pH effect probably because TMC was characterized by intrinsic solubility higher than that of CS, and moreover the mucoadhesive potential of TMC NP was stronger as previously stated (9).

Generally, nanoparticle absorption involves both paracellular and transcellular (endocytic) routes. Paracellular route utilizes less than 1% of the mucosal surface area. It has been reported that chitosan and its quaternized derivatives in nanoparticulate form are able to increase permeability through the opening of tight junctions (9,17). Furthermore, since endocytosis is a process initiated for nanoparticles by an unspecific physical adsorption of material to the cell surface by electrostatic forces and hydrogen bonding or hydrophobic interactions (17), TMC characterized by fixed positive charge might be better taken up in nanoparticulate form, counterbalancing the scarce interaction

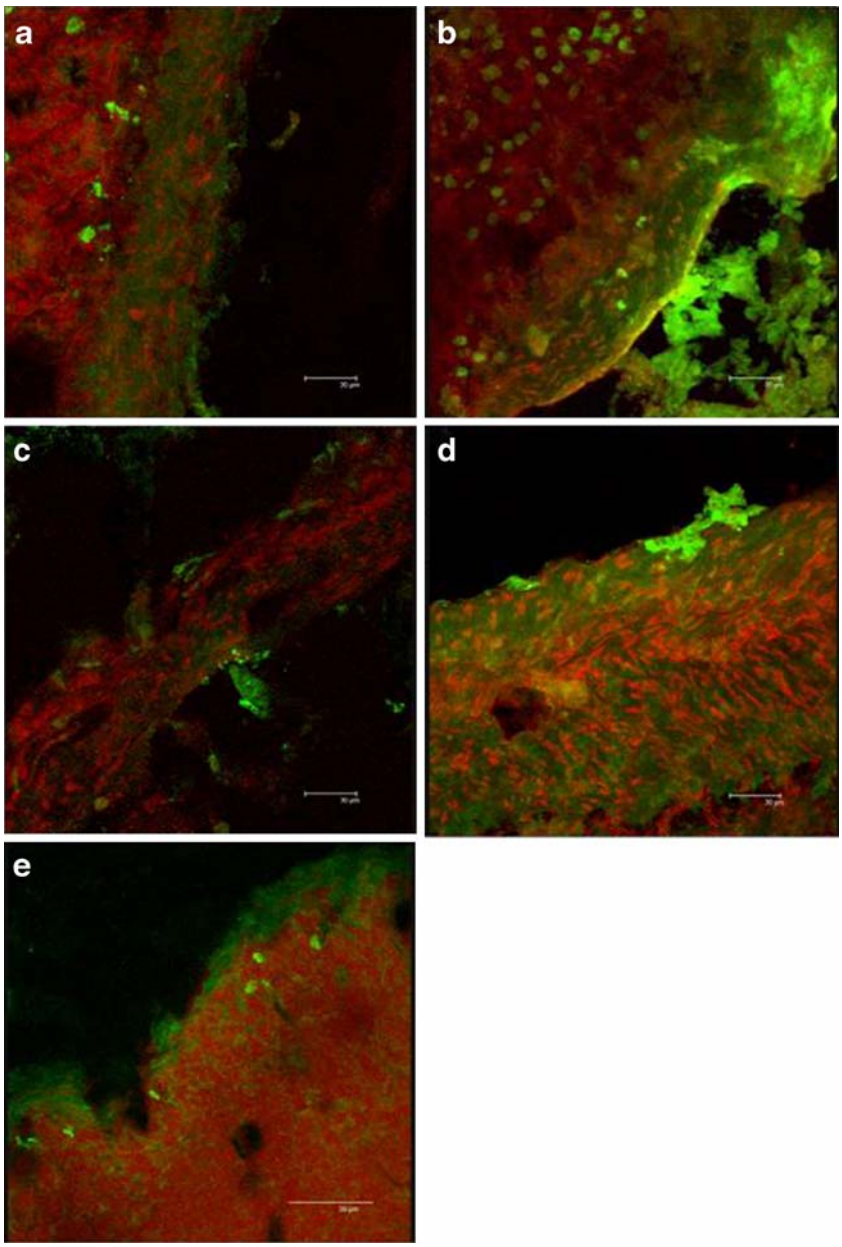

Fig. 8. CLSM microphotographs of the duodenum tissues treated with **a** ps CS; **b** NP CS; **c** ps TMC; **d** NP TMC; **e** insulin solution

with biologic substrate due to the poor flexibility of polymer chains (18,19).

The differences of results obtained using jejunum tract with respect to duodenum could be due to the peculiar properties of each tract considered: the intestine segments maintain mucus gel layer, covering the epithelium, with its microclimate pH poorly affected by luminal pH (20). It was also observed that in the *ex vivo* model used in the present work the tissues were covered by a continuously secreted layer of mucus that conceivably deeply affected the behavior of the tested systems.

Moreover, insulin at pH 5.5 is in unionized form because the pH is close to isoelectric point: this should produce higher absorption of the drug in the duodenum portion (also in the case of TMC solution) in the presence of polymers where the microclimate pH is close to 5.5, while in jejunum tract lower values of P_{app} could be seen probably because the secreting mucus layer was characterized by higher microclimate pH of 6–6.5.

In the ileum, both TMC NP and CS NP and polymer solutions were not able to improve insulin permeation. The failure of penetration enhancement on this part of intestine had been yet observed in a previous paper (21): this could be probably not only due to high environmental pH but also to the thicker mucus layer and to the rich enzymatic pool present in it.

The mucus layer on intestine tract has been considered a diffusion barrier to the transport of peptides due to possible interactions related to higher molecular weight and hydrophilicity (22). In a previous work on the role of mucus/glycocalyx on insulin intestinal absorption (23), it was stated that the intestinal epithelia did not impair diffusive paracellular and transcellular absorption, while the predominant barrier to insulin adsorption was the enzymatic barrier. In fact, the removal with hyaluronidase of mucus layer proved that insulin was degraded in this compartment (24), and coadministration of an enzyme inhibitor (aprotinin) increased insulin absorption, confirming the influence of brush-border membrane enzymes (25).

The P_{app} values obtained in *ex vivo* study were globally higher than those of *in vitro* study on Caco-2 cells. This was also evidenced by Bayat *et al.* (17). The reason for such behavior could be attributed to nanoparticle entrapment in

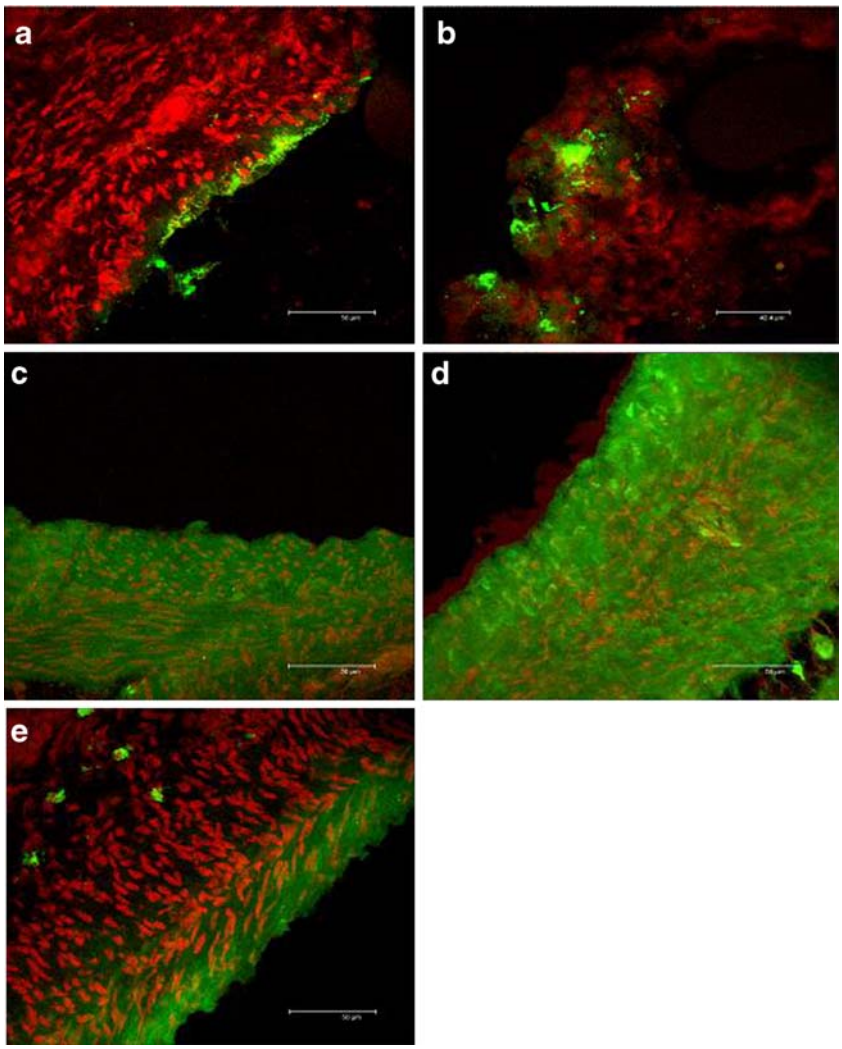

Fig. 9. CLSM microphotographs of the jejunum tissues treated with **a** ps CS; **b** NP CS; **c** ps TMC; **d** NP TMC; **e** insulin solution

mucus and to the presence of mucus and tissue enzymes which could cause nanoparticle digestion (17).

Figure 8 reports CLSM microphotographs of the duodenum tissues, maintained in contact during the permeation experiment, with: (a) CS ps, (b) CS nanoparticles, (c) TMC polymeric solution, (d) TMC nanoparticles, and (e) insulin solution.

In this case, information can be obtained about FL-INS remaining inside the tissue (penetration) at the end of permeation experiments.

The nuclei were stained using propidium iodide and appeared red, while the green fluorescence corresponds to the FL-INS. TMC and CS presented a similar behavior both as nanoparticles and as solutions. The tissue treated with polymer solutions showed a diffuse green fluorescence into the epithelial mucosa close to the nuclei (Fig. 8a, c). The substrates treated with both the nanoparticulate systems (Fig. 8b, d) presented a similar pattern: intense green fluorescence was evident in the epithelial zone between nuclei, and green spots with size comparable to that of nanoparticles were located close to the epithelium surface. Due to the mucoadhesive properties of CS and TMC, it seems that nanoparticles adhered to the intestinal walls, starting the promotion of insulin permeation as also stated by Sarmento *et al.* (26). The substrate treated with insulin solution (Fig. 8e) was characterized by slight fluorescence intensity principally localized on the epithelial surface outside the tissue probably in the mucus layer which covered duodenum.

Even if TMC and CS solutions were able to enhance the permeation of FL-INS to a greater extent with respect to the correspondent nanoparticulate forms (Fig. 7), FL-INS-loaded nanoparticles (green spots with intense fluorescence) were more efficiently entrapped into the duodenum tissue. This can be an explanation of the higher permeation of insulin observed in Fig. 6 promoted by CS solution with respect to CS NP. A different penetration enhancement mechanism was in fact probably involved. It is conceivable that NP were much more internalized by endocytosis, and in fact Fig. 8 evidenced that fluorescence inside the tissue was more intense for CS NP (a) with respect to CS solution (b).

Figure 9 reports CLSM microphotographs of the jejunum tissues, maintained in contact during the permeation experiment, with: (a) CS ps, (b) CS nanoparticles, (c) TMC polymeric solution, (d) TMC nanoparticles, and (e) insulin solution.

TMC and CS showed a behavior clearly different from that evidenced in duodenum tissue. In particular, after contact with both CS solution (Fig. 9a) and NP (Fig. 9b), green fluorescence was localized only on tissue surface while no fluorescence was present in the tissue depth; this could be due to a precipitation of CS solution which entrapped insulin molecules into entangled polymer chains, conferring the same behavior to chitosan solution and CS NP. On the contrary, the tissues maintained in contact with TMC NP (Fig. 9c) and TMC solution (Fig. 9d) were characterized by an intense green fluorescence in the whole tissue depth. In addition, the tissue maintained in contact with TMC NP (Fig. 9d) presented a round-shaped intense green fluorescence probably due to the nanoparticle entrapment into the tissue. These results confirmed that chitosan suffered environmental pH close to neutrality and although it was able to enhance FL-INS permeation, this effect was less evident in the jejunum than in duodenum portion. On the contrary, TMC maintained the penetration enhancement properties also at high pH values, and it demonstrated to be effective also as polymer solution. In the substrate treated with insulin solution (Fig. 9e), there was a slight fluorescence intensity which reached only few external cell layers.

CONCLUSIONS

CS and TMC demonstrated to be biocompatible both as solutions and in nanoparticulate form.

The *in vitro* model (Caco-2 cells) showed that CS and TMC were able to enhance insulin permeation both as NP and as solutions. CS NP were still able to widen paracellular pathways while TMC slightly interfered with substrate integrity.

The *ex vivo* model (mucus-secreting excised rat duodenum, jejunum, and ileum) put in evidence the role of mucus layer and of its microclimate pH, which could not be considered using Caco-2 model lacking mucus-secreting cells. CS and TMC solutions enhanced insulin permeation across duodenum much more than NP: duodenum pH favored chitosan, freely soluble in this environment, and consequently trimethylation of chitosan did not improve penetration enhancement properties.

TMC NP was more effective than CS NP and polymer solutions towards jejunum portion because of high mucoadhesive potential of TMC NP and because the pH of microclimate mucus environment (pH 6–6.5) was disadvantageous to CS. Both TMC and CS failed penetration enhancement towards ileum probably due to a thicker mucus layer with barrier properties and a rich enzyme pool. P_{app} values determined by means of *in vitro* model (Caco-2) were lower than those observed in *ex vivo* experiments because the tissue enzymes should cause NP digestion and consequently drug adsorption, and the mucus should favor a deep interaction with epithelial cells. The mechanism of penetration enhancement (evidenced also by CLSM analysis) involved paracellular pathway with an enlargement of tight junctions for polymer solutions and CS NP, while endocytosis/internalization into duodenum and jejunum epithelial cells was confirmed only for nanoparticulate form.

The good penetration enhancement properties (permeation and penetration/internalization) make TMC NP suitable carriers for oral administration of insulin.

REFERENCES

1. Aboubakar M, Couvreur P, Pinto-Alphandary H, Gouritin B, Lacur B, Farinotti R, *et al.* Insulin-loaded nanocapsules for oral administration: in vitro and *in vivo* investigation. Drug Dev Res. 2000;49:109–17.
2. Sadeghi AM, Dorkoosh FA, Avadi MR, Weinhold M, Bayat A, Delie F, *et al.* Permeation enhancer effect of chitosan and chitosan derivatives: comparison of formulations as soluble polymers and nanoparticulate systems on insulin absorption in Caco-2 cells. Eur J Pharm Biopharm. 2008;70:270–8.
3. Ponchel G, Montisci M-J, Dembri A, Durrer C, Duchene D. Mucoadhesion of colloidal particulate systems in the gastrointestinal tract. Eur J Pharm Biopharm. 1997;44:25–31.
4. Hans ML, Lowman AM. Biodegradable nanoparticles for drug delivery and targeting. Curr Opin Solid State Mater Sci. 2002; 6:319–27.
5. Janes KA, Calvo P, Alonso MJ. Polysaccharide colloidal particles as delivery systems for macromolecules. Adv Drug Del Rev. 2001;47:83–57.
6. Goycoolea FM, Lollo G, Remuñán-López C, Quaglia F, Alonso MJ. Chitosan-alginate blended nanoparticles as carriers for the

transmucosal delivery of macromolecules. Biomacromolecules. 2009;10:1736–43.
7. Kotzé AF, de Leeuw BJ, Lueßen HL, de Boer AG, Verhoef JC, Junginger HE. Chitosans for enhanced delivery of therapeutic peptides across intestinal epithelia: *in vitro* evaluation in Caco-2 cell monolayers. Int J Pharm. 1997;159:131–6.
8. Thanou M, Verhoef JC, Roemeijn SG, Nagelkerke JF, Merkus WH, Junginger HE. Effects of *N*-trimethyl chitosan chloride, a novel absorption enhancer, on Caco-2 intestinal epithelia and the ciliary beat frequency of chicken embryo trachea. Int J Pharm. 1999;185:73–8.
9. Sandri G, Bonferoni MC, Rossi S, Ferrari F, Gibin S, Zambito Y, *et al.* Nanoparticles based on *N*-trimethyl chitosan: evaluation of absorption properties using *in vitro* (Caco-2 cells) and *ex vivo* (excised rat jejunum) models. Eur J Pharm Biopharm. 2007; 65:78–67.
10. Sieval AB, Thanou M, Kotzè AF, Verhoef JC, Brussee J, Junginger HE. Preparation and NMR characterization of highly substituted *N*-trimethyl chitosan chloride. Carbohyd Res. 1998;36:175–65.
11. Di Colo G, Burgalassi S, Zambito Y, Monti D, Chetoni P. Effects of different *N*-trimethyl chitosans on *in vitro*/*in vivo* ofloxacin transcorneal permeation. J Pharm Sci. 2004;93:2851–62.
12. Calvo P, Remunan-Lopez C, Vila-Jato JL, Alonso MJ. Novel hydrophilic chitosan–polyethylene oxide nanoparticles as protein carriers. J Appl Polym Sci. 1997;63:125–32.
13. Dorkoosh FA, Verhoef JC, Ambagts MHC, Rafiee-Tehrani M, Borchard G, Junginger HE. Peroral delivery systems based on superporous hydrogel polymers: release characteristics for the peptide drugs buserelin, octreotide and insulin. Eur J Pharm Sci. 2002;15:433–9.
14. Dodane V, Amin Khan A, Mervin JR. Effect of chitosan on epithelial permeability and structure. Int J Pharm. 1999;182:21–32.
15. Smith J, Wood E, Dornish M. Effect of chitosan on epithelial cell tight junctions. Pharm Res. 2004;21:43–9.
16. Ma Z, Lim L-Y. Uptake of chitosan associated insulin in Caco-2 cell monolayers: a comparison between chitosan molecules and chitosan nanoparticles. Pharm Res. 2003;20:1812–9.
17. Bayat A, Dorkoosh FA, Dehpour AR, Moezi L, Larijani B, Junginger HE, *et al.* Nanoparticles of quaternized chitosan derivatives as a carrier for colon delivery of insulin: *ex vivo* and *in vitro* study. Int J Pharm. 2008;356:259–66.
18. Yin L, Ding J, He C, Cui L, Tang C, Yin C. Drug permeability and mucoadhesion properties of thiolated trimethyl chitosan nanoparticles in oral insulin delivery. Biomaterials. 2009;30:5691–700.
19. Jonker C, Hamman JH, Kotze AF. Intestinal paracellular permeation enhancement with quaternized chitosan: *in situ* and *in vitro* evaluation. Int J Pharm. 2002;238:205–13.
20. Lee K-J, Johnson N, Castelo J, Sinko PJ, Grass G, Holme K, *et al.* Effect of experimental pH on the *in vitro* permeability in intact rabbit intestines and Caco-2 monolayer. Eur J Pharm Sci. 2005;25:193–200.
21. Horter D, Dressman JB. Influence of physicochemical properties on dissolution of drugs in the gastrointestinal tract. Adv Drug Deliv Rev. 1997;25:3–14.
22. Schillin RJ, Mitra AK. Intestinal mucosal transport of insulin. Int J Pharm. 1990;62:53–64.
23. Aoki Y, Morishita M, Asai K, Akikusa B, Hosoda S, Takayama K. Region-dependent role of the mucous/glycocalyx layers in insulin permeation across rat small intestinal membrane. Pharm Res. 2005;22:1854–62.
24. Aoki Y, Morishita M, Takayama K. Role of the mucous/glycocalyx layers in insulin permeation across the rat ileal membrane. Int J Pharm. 2005;297:98–109.
25. Morishita M, Aoki Y, Sakagami M, Nagai T, Takayama K. *In situ* ileal absorption of insulin in rats: effects of hyaluronidase pretreatment diminishing the mucous/glycocalyx layers. Pharm Res. 2004;21:309–16.
26. Sarmento B, Ribeiro A, Veiga F, Ferreira D, Neufeld R. Oral bioavailability of insulin contained in polysaccharide nanoparticles. Biomacromolecules. 2007;8:3054–60.